CHAPTER IV
RESULTS AND DISCUSSION

Generally, in a plasma environment, the generation of strongly energetic electrons can occur from the collision between the gliding arc discharge and the gaseous molecules of hydrocarbons, CO_2, O_2, and H_2O, creating a variety of chemically active radicals. All the possibilities of chemical pathways occurring under the studied conditions are briefly described below to provide a better comprehensive understanding of the combined steam reforming and partial oxidation of CO_2-containing natural gas in gliding arc discharge plasma. The radicals of oxygen-active species are produced during the collisions between electrons and CO_2, as shown in Equations 4.1 and 4.2. Moreover, the produced CO can be further dissociated by the collisions with electrons to form coke and oxygen-active species (Equation 4.3). In the case of added oxygen, a large amount of oxygen-active species can be produced from the collisions between electrons and oxygen molecules, as described by Equations 4.4-4.6. The collisions between electrons and all hydrocarbons presented in the feed to produce hydrogen and various hydrocarbon species for subsequent reactions are described by Equations 4.7-4.19.

Electron-carbon dioxide collisions:

$$e^- + CO_2 \rightarrow CO + O^- \quad (4.1)$$

$$e^- + CO_2 \rightarrow CO + O + e^- \quad (4.2)$$

$$e^- + CO \rightarrow C + O + e^- \quad (4.3)$$

Electron-oxygen collisions:

$$e^- + O_2 \rightarrow 2O + e^- \rightarrow O^- + O \quad (4.4)$$

$$e^- + O_2 \rightarrow O_2^- \quad (4.5)$$

$$e^- + O_2 \rightarrow 2O + e^- \quad (4.6)$$

Electron-methane collisions:

$$e^- + CH_4 \rightarrow CH_3 + H + e^- \quad (4.7)$$

$$e^- + CH_3 \rightarrow CH_2 + H + e^- \quad (4.8)$$

$$e^- + CH_2 \rightarrow CH + H + e^- \quad (4.9)$$

$$e^- + CH \rightarrow C + H + e^- \quad (4.10)$$

$$H + H \rightarrow H_2 \quad (4.11)$$

Electron-ethane collisions:

$$e^- + C_2H_6 \rightarrow C_2H_5 + H + e^- \quad (4.12)$$

$$e^- + C_2H_5 \rightarrow C_2H_4 + H + e^- \quad (4.13)$$

$$e^- + C_2H_4 \rightarrow C_2H_3 + H + e^- \quad (4.14)$$

$$e^- + C_2H_3 \rightarrow C_2H_2 + H + e^- \quad (4.15)$$

$$e^- + C_2H_6 \rightarrow CH_3 + CH_3 + e^- \quad (4.16)$$

Electron-propane collisions:

$$e^- + C_3H_8 \rightarrow C_3H_7 + H + e^- \quad (4.17)$$

$$e^- + C_3H_7 \rightarrow C_3H_6 + H + e^- \quad (4.18)$$

$$e^- + C_3H_8 \rightarrow C_2H_5 + CH_3 + e^- \quad (4.19)$$

The oxygen-active species derived from CO_2 and O_2 can further extract hydrogen atoms from the molecules of hydrocarbon gases via the oxidative dehydrogenation reactions (Equations 4.20-4.33), consequently producing several chemically active radicals and water.

Oxidative dehydrogenation reactions:

$$CH_4 + O \rightarrow CH_3 + OH \quad (4.20)$$

$$C_2H_6 + O \rightarrow C_2H_5 + OH \quad (4.21)$$

$$C_2H_5 + O \rightarrow C_2H_4 + OH \quad (4.22)$$

$$C_2H_4 + O \rightarrow C_2H_3 + OH \quad (4.23)$$

$$C_2H_3 + O \rightarrow C_2H_2 + OH \quad (4.24)$$

$$C_3H_8 + O \rightarrow C_3H_7 + OH \quad (4.25)$$

$$C_3H_7 + O \rightarrow C_3H_6 + OH \quad (4.26)$$

$$CH_4 + OH \rightarrow CH_3 + H_2O \quad (4.27)$$

$$C_2H_6 + OH \rightarrow C_2H_5 + H_2O \quad (4.28)$$

$$C_2H_5 + OH \rightarrow C_2H_4 + H_2O \quad (4.29)$$

$$C_2H_4 + OH \rightarrow C_2H_3 + H_2O \quad (4.30)$$

$$C_2H_3 + OH \rightarrow C_2H_2 + H_2O \quad (4.31)$$

$$C_3H_8 + OH \rightarrow C_3H_7 + H_2O \quad (4.32)$$

$$C_3H_7 + OH \rightarrow C_3H_6 + H_2O \quad (4.33)$$

The C_2H_5, C_2H_3, and C_3H_7 radicals can further react to form ethylene, acetylene, and propene either by electron collision (Equations 4.13-4.15, and 4.18) or by oxidative dehydrogenation reaction (Equations 4.22-4.24, 4.26-4.29, 4.31, and 4.33). The extracted hydrogen atoms immediately form hydrogen gas according to Equation 4.11. However, no propene is detected in the outlet gas stream. It is therefore believed that the propene species is unstable and may possibly undergo further reactions (Equations 4.34 and 4.35).

Propene hydrogenation and cracking reactions:

$$C_3H_6 + H_2 \rightarrow C_3H_8 \quad (4.34)$$

$$C_3H_6 \rightarrow C_2H_2 + CH_4 \quad (4.35)$$

In addition, the radicals of hydrocarbons and hydrogen derived from the earlier reactions react further to combine with one another to form ethane, ethylene, acetylene, propane, and butane, as shown in Equations 4.36-4.51. In addition, ethane can be further dehydrogenated to form ethylene, while ethylene can also be dehydrogenated to form acetylene by either electron collision or oxidative dehydrogenation (Equations 4.12, 4.13, 4.21, 4.22, 4.28, and 4.29 for ethylene formation; and, Equations 4.14, 4.15, 4.23, 4.24, 4.30, and 4.31 for acetylene formation).

Coupling reactions of active species:

Ethane formation;

$$CH_3 + CH_3 \rightarrow C_2H_6 \quad (4.36)$$

$$C_2H_5 + H \rightarrow C_2H_6 \quad (4.37)$$

$$C_2H_5 + C_2H_5 \rightarrow C_2H_6 + C_2H_4 \quad (4.38)$$

$$C_3H_7 + CH_3 \rightarrow C_2H_6 + C_2H_4 \quad (4.39)$$

Ethylene formation; $CH_2 + CH_2 \rightarrow C_2H_4$ (4.40)

$CH_3 + CH_3 \rightarrow C_2H_4 + H_2$ (4.41)

$C_2H_5 + H \rightarrow C_2H_4 + H_2$ (4.42)

$C_3H_7 + H \rightarrow C_2H_4 + CH_4$ (4.43)

Acetylene formation; $CH + CH \rightarrow C_2H_2$ (4.44)

$CH_2 + CH_2 \rightarrow C_2H_2 + H_2$ (4.45)

$CH_3 + CH \rightarrow C_2H_2 + H_2$ (4.46)

$C_2H_5 + H \rightarrow C_2H_2 + H_2 + H_2$ (4.47)

$C_3H_7 + H \rightarrow C_2H_2 + CH_4 + H_2$ (4.48)

Propane formation; $C_2H_5 + CH_3 \rightarrow C_3H_8$ (4.49)

Butane formation; $C_2H_5 + C_2H_5 \rightarrow C_4H_{10}$ (4.50)

$C_3H_7 + CH_3 \rightarrow C_4H_{10}$ (4.51)

Moreover, a significant amount of CO and a very small amount of water are produced under the studied conditions, particularly in feed with high oxygen content derived from CO_2 dissociation. CO may be mainly formed via the CO_2 dissociation (Equations 4.1 and 4.2). Equations 4.52-4.56 show the partial oxidative pathways of methane to form CO and H_2 as the end products. The formation of water is believed to occur via the oxidative hydrocarbon reactions (Equations 4.27-4.33). In addition, water can be formed by the reactions between hydrogen or active hydrogen radical and active oxygen radical, as shown in Equations 4.57-4.59.

Carbon monoxide formation:

$CH_3 + O \rightarrow HCHO$ (4.52)

$HCHO + O \rightarrow OH + CHO$ (4.53)

$CHO + O \rightarrow OH + CO$ (4.54)

$CHO + OH \rightarrow CO + H_2O$ (4.55)

$CHO + H \rightarrow H_2 + CO$ (4.56)

Water formation:

$$2H + O \rightarrow H_2O \quad (4.57)$$

$$H_2 + O \rightarrow H_2O \quad (4.58)$$

$$H_2 + \tfrac{1}{2} O \rightarrow H_2O \quad (4.59)$$

Additionally, hydrocarbon molecules may crack to form carbon and hydrogen via thermal cracking reactions (Equations 4.60-4.62).

$$CH_4 \rightarrow C + 2H_2 \quad (4.60)$$

$$C_2H_6 \rightarrow 2C + 3H_2 \quad (4.61)$$

$$C_3H_8 \rightarrow 3C + 4H_2 \quad (4.62)$$

Moreover, water molecule may crack to form hydrogen via dissociation reactions (Equations 63-64).

$$e^- + H_2O \rightarrow O^- + H_2 \quad (4.63)$$

$$e^- + H_2O \rightarrow OH^- + H \quad (4.64)$$

4.1 The Effect of Stage Number of Plasma Reactors

In general, the probability of collisions between reactant molecules and highly energetic electrons in plasma system is governed by both residence time and stage number of plasma reactors (Rueangjitt, 2009). In order to identify the effects of residence time and stage number of plasma reactors, the series of experiments were divided into two sets. Firstly, the effect of residence time at a constant total feed flow rate was investigated to evaluate how it affected the process performance. The experiments were performed by varying residence time at a constant total feed flow rate of 100 cm^3/min, while the other operating parameters were controlled at the base conditions of a steam content of 10 mol%, an input voltage of 14.5 kV, an input frequency of 300 Hz, and an electrode gap distance of 6 mm (Pornmai, 2012). The residence time of the single stage, 2, 3, and 4 stages was controlled at 1.37, 2.71, 4.11, and 5.48 s, respectively. Secondly, to investigate the effect of the stage number of plasma reactors, the experiments were performed at the fixed residence time of 4.11 s, whereas the other operating parameters were controlled at the base conditions,

as mentioned above. For each stage of plasma reactor, the total feed flow rate was controlled at 33.3, 66.6, 100, and 133.3 cm^3/min, respectively, in order to maintain the same residence time of 4.11 s.

4.1.1 Effect on Reactant Conversions and Product Yields

4.1.1.1 Constant Total Feed Flow Rate

Figure 4.1a illustrates the influence of the residence time on the reactant conversions and product yields at a constant total feed flow rate. The results show that all reactant conversions tended to remarkably increase with increasing stage number of plasma reactors, especially the C_3H_8 conversion. It was supported by the concentrations of outlet gas that the C_3H_8 concentration sharply decreased, while the CH_4, C_2H_6, CO_2, and O_2 concentrations gradually decreased (Figure 4.2a). Generally, the probability of collisions between reactant molecules and highly energetic electrons is governed by "contact time" or "residence time". As a result, a higher opportunity for reactants to be collided with highly energetic electrons in the plasma reaction zone can be obtained at a higher residence time. Therefore, increasing residence time brings about increases in all reactant conversions. In addition, the significant increase in the C_3H_8 conversion as compared to the others, as mentioned above, can be clarified by their bond dissociation energies (Perrey, 1997). Surprisingly, the CO_2 conversion was found to have a positive value of about 7.78 % when increasing residence time from 2.71 to 4.11 s (2 to 3 stages of plasma reactors), which is different from the previous work (Rueangjitt, 2009). This can be explained in that the combined plasma steam reforming and partial oxidation plays an important role in enhancing the CO_2 conversion. Furthermore, the CO yield dramatically increased with increasing residence time from 1.37 to 5.48 s (from 1 to 4 stages of plasma reactors), whereas the C_2 yield remained almost unchanged (Figure 4.1a). In the meantime, the H_2 yield initially increased with increasing residence time from 1.37 to 2.74 s (1 to 2 stages of plasma reactors), and then remained almost unchanged with increasing residence time. The results indicate that the coupling reactions of the active species to produce CO are governed by residence time (Equations 6.52-6.56).

4.1.1.2 Constant Residence Time

The reactant conversions and product yields as a function of stage number of plasma reactors when varying total feed flow rate at a constant residence time of 4.11 s are depicted in Figure 4.1b. The results reveal that the CH_4 and C_2H_6 conversions and the C_2 yield remained almost unchanged with increasing stage number of plasma reactors, while the C_3H_8 conversion tended to primarily increase and then remained almost unchanged. Besides, the CO_2 conversion and the CO yield tended to increase with increasing stage number of plasma reactors from 1 to 3 stages, and then declined to have negative values with increasing stage number of plasma reactors from 3 to 4 stages. The explanation is that CO_2 is also a carbon source to produce the CO in the reforming process, as shown in electron-carbon dioxide collisions (Equations 4.1-4.3).

It is interesting to note that as compared to the CO_2 conversion, the O_2 conversion shows the opposite trend when increasing stage number of plasma reactors from 3 to 4 stages. This might be attributed to the consumption of O_2 to reproduce CO_2. Besides, it was found that increasing stage number of plasma reactors from 1 to 4 stages had an insignificant impact on the H_2 yield, which agrees well with the H_2 concentration in the outlet gas (Figure 4.2b). It can be implied that the H_2 yield was independent of stage number of plasma reactors in the investigated range.

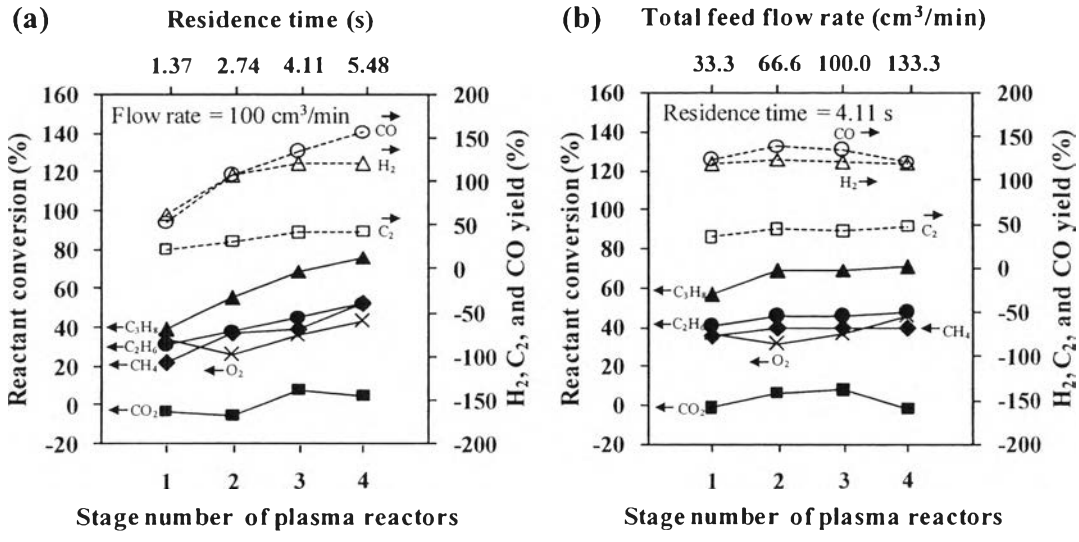

Figure 4.1 Effect of stage number of plasma reactors on reactant conversions and product yields for the combined steam reforming and partial oxidation of natural gas (a) at a constant total feed flow rate of 100 cm^3/min and (b) at a constant residence time of 4.11 s (steam content, 10 mol%; input voltage, 14.5 kV; input frequency, 300 Hz; and electrode gap distance, 6 mm).

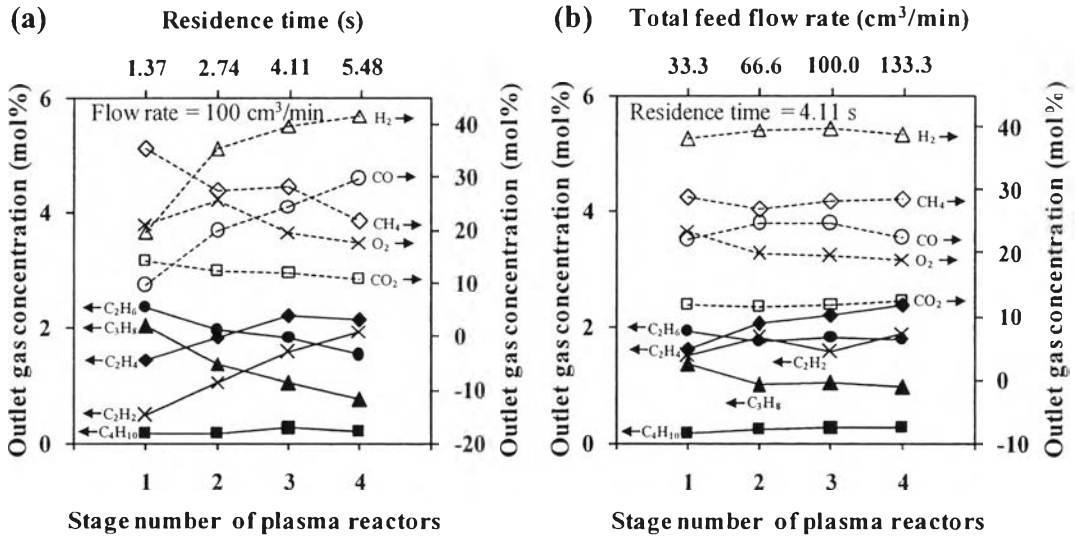

Figure 4.2 Effect of stage number of plasma reactors on concentrations of outlet gas for the combined steam reforming and partial oxidation of natural gas (a) at a constant total feed flow rate of 100 cm^3/min and (b) at a constant residence time of 4.11 s (steam content, 10 mol%; input voltage, 14.5 kV; input frequency, 300 Hz; and electrode gap distance, 6 mm).

4.1.2 Effect on Product Selectivities and Product Molar Ratios

4.1.2.1 Constant Total Feed Flow Rate

The effect of stage number of plasma reactors on the product selectivities at a constant total feed flow rate of 100 cm^3/min is shown in Figure 4.3a. When increasing residence time from 1.37 to 5.48 s (1 to 4 stages of plasma reactors), the C_2H_2 and CO selectivities tended to significantly increase, whereas the C_2H_4 and C_4H_{10} selectivities gradually decreased. These results correspond well with the decreases in C_2H_4/C_2H_2, H_2/C_2H_2, H_2/CO molar ratios (Figure 4.4a). The results infer that the opportunity for both the oxidative dehydrogenation reactions and coupling reactions of active species to form C_2H_2, H_2, and CO is more favorable in this range of residence time. It is interesting to mention that the H_2 selectivity dramatically increased when increasing residence time from 1.37 to 2.74 s (1 to 2 stages of plasma reactors), and then gradually decreased with further increasing residence time in the investigated range. It is possibly due to increasing consumption of H_2 to some extent to produce C_2H_2 with increasing residence time from 2.74 to 5.48 s (2 to 4 stages of plasma reactors).

4.1.2.2 Constant Residence Time

Figure 6.3b shows the effect of stage number of plasma reactors on the product selectivities at a constant residence time of 4.11 s. The selectivities for both H_2 and CO gradually decreased with increasing stage number of plasma reactors (1 to 4 stages). It is known that increasing stage number of plasma reactors results in a higher probability of the reactions of feed reactant molecules, product molecules formed in the previous reactors, as well as active species, leading to the increase in probability of coupling reactions. On the other hand, the selectivities for C_2H_4 and C_4H_{10} slightly increased with increasing stage number of plasma reactors, corresponding to the decreases in H_2/C_2H_4 and H_2/C_2H_2 molar ratios, whereas the C_2H_4/C_2H_2 molar ratio increased (Figure 6.4b). These results confirm that the coupling reactions of active species to form higher hydrocarbon products are likely to occur when increasing stage number of plasma reactors, which are different from the case of constant total feed flow rate. Besides, it is found that increasing stage number of plasma reactors has a insignificant impact on the C_2H_2 selectivity.

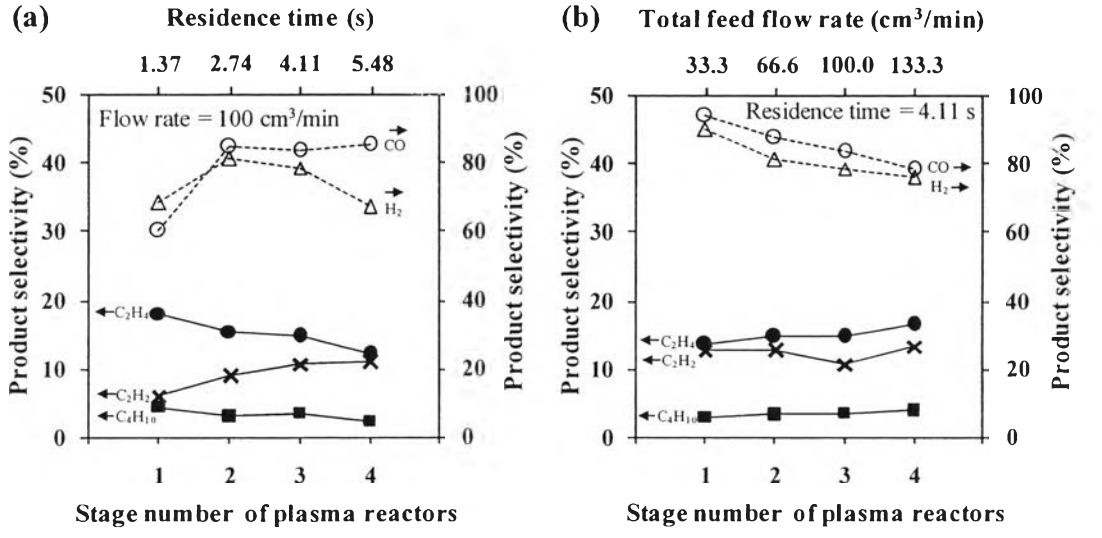

Figure 4.3 Effect of stage number of plasma reactors on product selectivities for the combined steam reforming and partial oxidation of natural gas (a) at a constant total feed flow rate of 100 cm^3/min and (b) at a constant residence time of 4.11 s (steam content, 10 mol%; input voltage, 14.5 kV; input frequency, 300 Hz; and electrode gap distance, 6 mm).

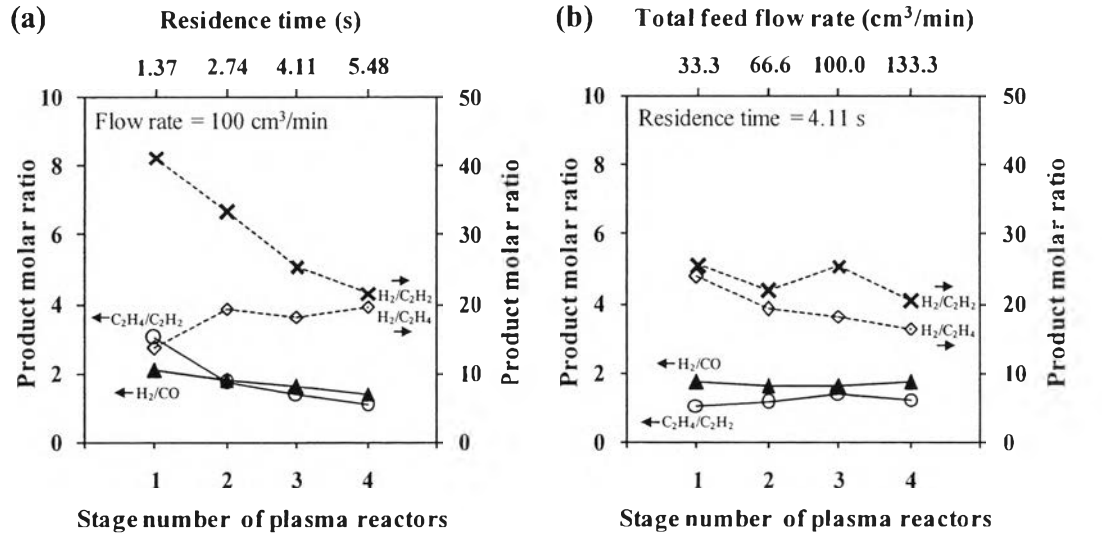

Figure 4.4 Effect of stage number of plasma reactors on product molar ratios for the combined steam reforming and partial oxidation of natural gas (a) at a constant total feed flow rate of 100 cm^3/min and (b) at a constant residence time of 4.11 s (steam content, 10 mol%; input voltage, 14.5 kV; input frequency, 300 Hz; and electrode gap distance, 6 mm).

4.1.3 Effect on Power Consumptions and Coke Formation

4.1.3.1 Constant Total Feed Flow Rate

As depicted in Figure 4.5a, the gradual decreases in the power consumptions per molecule of both reactants converted and hydrogen produced with increasing residence time from 1.37 to 4.11 s (1 to 3 stages of plasma reactors) was observed, and after that it slightly increased. Not surprisingly, coke formation tended to gradually increase with increasing residence time, resulting from higher opportunity for reactant molecules to be collided with highly energetic electrons, as mentioned above. The minimum power consumptions were 3.49×10^{-17} Ws per molecule of reactants converted and 2.04×10^{-17} Ws per molecule of hydrogen produced at 3 stages of plasma reactors.

4.1.3.2 Constant Residence Time

The effect of stage number of plasma reactors on power consumptions and coke formation at a constant residence time of 4.11 s is illustrated in Figure 4.5b. It can be clearly seen that the power consumptions per molecule of both reactants converted and hydrogen produced tended to dramatically decease with increasing stage number of plasma reactors from 1 to 3 stages, and then slightly increased. By comparing the case of constant total feed flow rate with that of constant residence time, increasing stage number of plasma reactors at a constant residence time results in an increase in power consumptions. However, the minimum power consumptions were found at the same conditions with 3 stages of plasma reactors. It is interesting to note that the coke formation tended to gradually decrease with increasing stage number of plasma reactors.

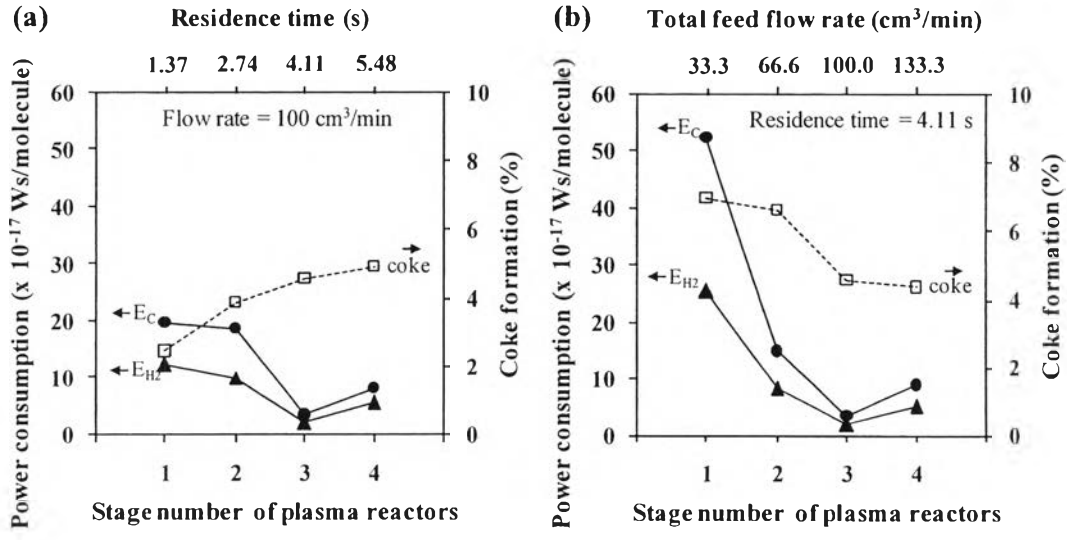

Figure 4.5 Effect of stage number of plasma reactors on power consumptions and coke formation for the combined steam reforming and partial oxidation of natural gas (a) at a constant total feed flow rate of 100 cm^3/min and (b) at a constant residence time of 4.11 s (steam content, 10 mol%; input voltage, 14.5 kV; input frequency, 300 Hz; and electrode gap distance, 6 mm).

4.2 The Effect of Hydrocarbons (HCs)/O_2 Feed Molar Ratio

In general, the feed composition plays a significant role on plasma behaviors, leading to the changes in plasma chemical reaction performance. For the examined plasma system, the experiments were performed by varying HCs/O_2 feed molar ratio at 2/1, 3/1, and 6/1. It should be noted that a HCs/O_2 feed molar ratio lower than 2/1 was not investigated in this plasma reactor since it is close to the explosion zone. In order to clarify the effect of HCs/O_2 feed molar ratio, the only simulated natural gas was used, while the other operating parameters were controlled at a steam content of 10 mol%, a total feed flow rate of 100 cm^3/min, an input voltage of 13.5 kV, an input frequency of 300 Hz, an electrode gap distance of 6 mm, and 3 stages of plasma reactors.

4.2.1 Effect on Reactant Conversions and Product Yields

Figure 4.6 shows the effect of HCs/O_2 feed molar ratio on the reactant conversions and product yields. The results reveal that all reactant conversions decreased with increasing HCs/O_2 feed molar ratio (the higher HCs/O_2 feed molar ratio, the lower oxygen content in feed). In order to better understand, it is worth describing a number of possible pathways for plasma to activate oxygen molecules that occur under the studied conditions.

It can be clearly seen that the increase in O_2 content in feed provides a higher oxygen-active species (Equations 4.4-4.6), leading to increasing an opportunity of oxidative dehydrogenation reactions of oxygen-active species. Thus, all reactant conversions show the decreasing tendency when increasing HCs/O_2 feed molar ratio. This explanation can also be used to explain the decreases in H_2 and CO yields when increasing HCs/O_2 feed molar ratio. Additionally, O_2 is considered to be an oxygen source to produce CO, so the decrease in O_2 content in feed directly diminishes coupling reactions of carbon monoxide formation (Equations 4.1-4.3). In addition, the C_2 yield slightly changed with increasing HCs/O_2 feed molar ratio.

Furthermore, the addition of O_2 in feed leads to the improvement of the CH_4, C_2H_6, and CO_2 conversions, as well as the CO yield, even with low O_2 content in feed (i.e. the HCs/O_2 feed molar ratio of 6/1). The O_2 addition in feed with the HCs/O_2 feed molar ratio of 2/1 potentially contributes to the enhancement of all the reactant conversions (except C_3H_8) and the CO yield, whereas slight changes were found for the H_2 and C_2 yields.

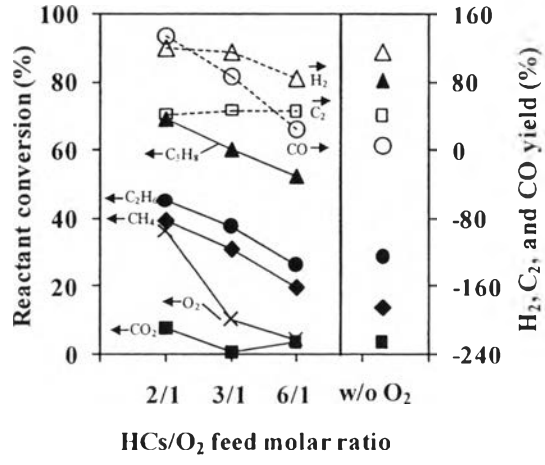

Figure 4.6 Effect of HCs/O_2 feed molar ratio on reactant conversions and product yields for the combined steam reforming and partial oxidation of natural gas (3 stages of plasma reactors; steam content, 10 mol%; total feed flow rate, 100 cm^3/min; input voltage, 14.5 kV; input frequency, 300 Hz; and electrode gap distance, 6 mm).

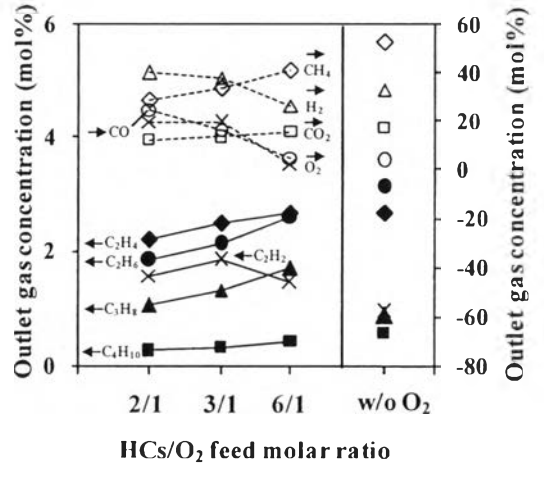

Figure 4.7 Effect of HCs/O_2 feed molar ratio on concentrations of outlet gas for the combined steam reforming and partial oxidation of natural gas (3 stages of plasma reactors; steam content, 10 mol%; total feed flow rate, 100 cm^3/min; input voltage, 14.5 kV; input frequency, 300 Hz; and electrode gap distance, 6 mm).

4.2.2 Effect on Product Selectivities and Product Molar Ratios

The effect of HCs/O_2 feed molar ratio on the product selectivities is depicted in Figures 4.8. The CO selectivity dramatically decreases with increasing HCs/O_2 feed molar ratio (decreasing O_2 content). An increase in O_2 content in the feed (decreasing HCs/O_2 feed molar ratio) provides excess amount of O and OH active species, causing an increase in possibility of the partial oxidative pathways forming CO as an end product (Equations 4.52-4.56). In contrast, the C_2H_2, C_2H_4, C_4H_{10} and H_2 selectivities tended to increase with increasing HCs/O_2 feed molar ratio. The results agree well with the previous work (Pornmai, 2012). The lower the HCs/O_2 feed molar ratio, the higher the number of oxygen-active species, subsequently increasing the opportunity for oxidative dehydrogenation reactions (Equations 4.20-4.33). As a result, several intermediate species (i.e. CH_3, C_2H_5, and C_3H_7) can further react to form H_2, C_2H_2, and C_2H_4 either by electron collisions or by oxidative dehydrogenation reactions (Equations 4.22 and 4.24). These results infer that the opportunity for coupling reactions to form H_2, C_2H_2, C_2H_4, and C_4H_{10} is less favorable at a lower HCs/O_2 feed molar ratio.

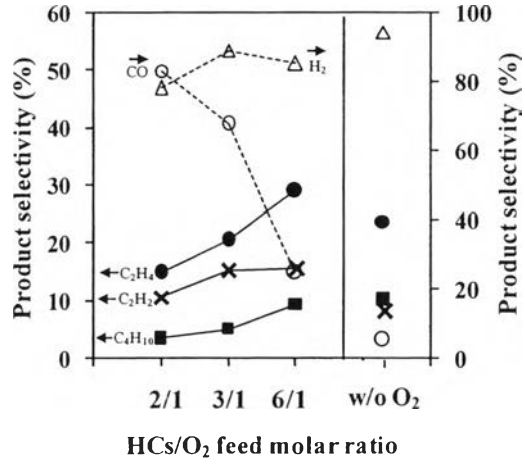

Figure 4.8 Effect of HCs/O_2 feed molar ratio on product selectivities for the combined steam reforming and partial oxidation of natural gas (3 stages of plasma reactors; steam content, 10 mol%; total feed flow rate, 100 cm^3/min; input voltage, 14.5 kV; input frequency, 300 Hz; and electrode gap distance, 6 mm).

Figure 4.9 shows the effect of HCs/O_2 feed molar ratio on the product molar ratios. Decreases in H_2/C_2H_2 and H_2/C_2H_4 molar ratios with increasing HCs/O_2 feed molar ratio imply that the increase in the C_2H_2 and C_2H_4 production rates is higher than that of the H_2 production rate. Interestingly, the H_2/CO molar ratio was found to increase sharply with increasing HCs/O_2 feed molar ratio (HCs/O_2 molar ratio of 1.62 at HCs/O_2 of 2/1, 2.33 at HCs/O_2 of 3/1, 5.81 at HCs/O_2 of 6/1, and 28.25 at without oxygen addition in feed). Hence, the HCs/O_2 feed molar ratio can be considered to be a key factor for determining the ratio of synthesis gas (H_2/CO) in this plasma system. Moreover, the C_2H_4/C_2H_2 molar ratio was found to slightly change with increasing HCs/O_2 feed molar ratio.

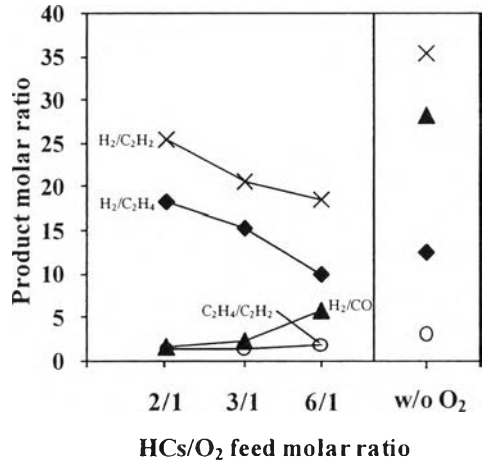

Figure 4.9 Effect of HCs/O_2 feed molar ratio on product molar ratios for the combined steam reforming and partial oxidation of natural gas (3 stages of plasma reactors; steam content, 10 mol%; total feed flow rate, 100 cm^3/min; input voltage, 14.5 kV; input frequency, 300 Hz; and electrode gap distance, 6 mm).

4.2.3 Effect on Power Consumptions and Coke Formation

As shown in Figure 4.10, the power consumptions both per reactant molecule converted and per H_2 molecule produced significantly increased with increasing HCs/O_2 feed molar ratio. The decreasing tendencies in both power consumptions can be described by the increases in the CH_4, C_2H_6, and C_3H_8 conversions and the H_2 yield (Figure 4.6). In addition, coke formation only slightly

changed with increasing HCs/O_2 feed molar ratio, suggesting that it was independent of O_2 content in the investigate range.

By comparing between the cases with and without of oxygen addition in feed, it was clearly seen that the presence of oxygen in feed plays an important role in enhancing the reactant conversions (except C_3H_8), the CO and H_2 yields, the power consumptions both per reactant molecule converted and per H_2 molecule produced, as well as the decrease in carbon deposition on the electrode surfaces. However, higher hydrocarbons (i.e. C_2H_2, C_2H_4, and C_4H_{10}) are likely to form at a low oxygen content. From the overall results, the optimum HCs/O_2 feed molar ratio of 2/1 was selected for further investigation.

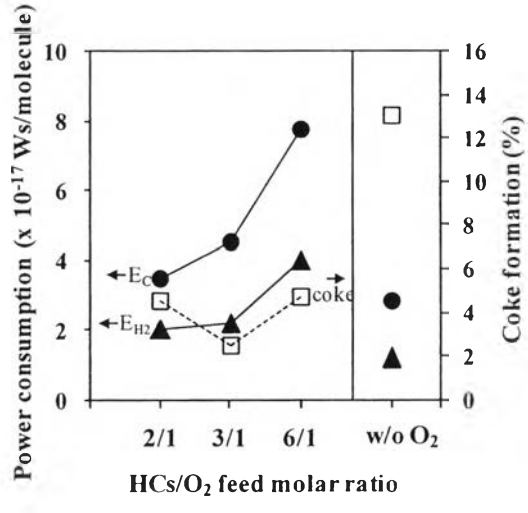

Figure 4.10 Effect of HCs/O_2 feed molar ratio on power consumptions and coke formation for the combined steam reforming and partial oxidation of natural gas (3 stages of plasma reactors; steam content, 10 mol%; total feed flow rate, 100 cm^3/min; input voltage, 14.5 kV; input frequency, 300 Hz; and electrode gap distance, 6 mm).

4.3 Effect of Input Voltage

Input voltage and frequency are technically considered as key parameters in operating the plasma chemical processing and sustaining the plasma stability. However, based on the previous work (Rueangjitt, 2008), the input frequency of 300 Hz was proved to be an optimum value for CO_2-containing natural

gas reforming using gliding arc discharge. Hence, the input frequency of 300 Hz was selected for investigating the effect of input voltage in this present work. To examine the effect of input voltage on the combined plasma steam reforming and partial oxidation of CO_2-containing natural gas in a multistage gliding arc system, the input voltage was varied in the rage of 13.5-16.8 kV, while the total feed flow rate, HCs/O_2 feed molar ratio, input frequency, and electrode gap distance were kept constant.

4.3.1 Effect on Reactant Conversions and Product Yields

As shown in Figure 4.11, all of reactant conversions (except CO_2) remained almost unchanged with increasing input voltage. The results suggest that the CH_4, C_2H_6, and C_3H_8 conversions were independent of input voltage in these investigate ranges. Nevertheless, in this plasma system, the input voltage higher than 16.8 kV rapidly provided a very large amount of coke deposited on the electrode surface, leading to the instability and thereby the extinction of gliding arc discharge. In contrast, the lowest operating input voltage of 13.5 kV was limited by the breakdown voltage, which is the minimum value of voltage required to create the steady plasma environment. It is interesting to note that the CO_2 conversion remained unchanged with increasing input voltage from 13.5 to 14.5 kV, then dramatically increase with increasing input voltage from 14.5 to 15 kV, and finally slightly changed with further increasing input voltage to 16.8 kV, implying that the input voltage of 15 kV is considered to be the optimum value. As expected, the H_2 and C_2 yields gradually increased with increasing input voltage. In general, an increase in input voltage leads to a stronger electric field strength across the electrodes, contributing to a higher electron density. Since a higher electron density results in a higher average energy and temperature of electrons, the opportunity for the occurrence of elementary chemical reactions with electron impact is improved.

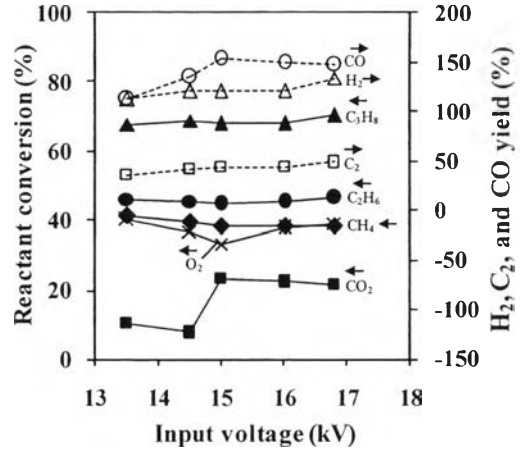

Figure 4.11 Effect of input voltage on reactant conversions and product yields for the combined steam reforming and partial oxidation of natural gas (3 stages of plasma reactors; steam content, 10 mol%; HCs/O_2 feed molar ratio of 2/1; total feed flow rate, 100 cm^3/min; input frequency, 300 Hz; and electrode gap distance, 6 mm).

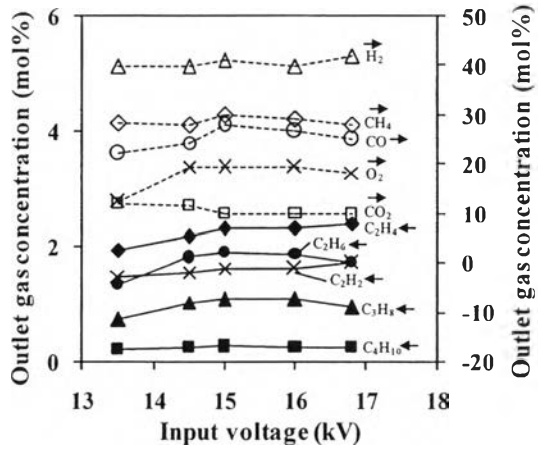

Figure 4.12 Effect of input voltage on concentrations of outlet gas for the combined steam reforming and partial oxidation of natural gas (3 stages of plasma reactors; steam content, 10 mol%; HCs/O_2 feed molar ratio of 2/1; total feed flow rate, 100 cm^3/min; input frequency, 300 Hz; and electrode gap distance, 6 mm).

4.3.2 Effect on Product Selectivities and Product Molar Ratios

Figure 4.13 shows the effect of input voltage on the product selectivities. The selectivities for C_2H_2, C_2H_4, and H_2 gradually increased with increasing input voltage, whereas the C_4H_{10} selectivity remained almost unchanged. As described earlier, the influence of the greater electron density results in boosting

the collisions between reacting gas molecules and energetic electrons, leading to the increase in the product formation. In addition, the H_2/C_2H_2 and H_2/C_2H_4 molar ratios slightly declined with increasing input voltage, while the C_2H_4/C_2H_2 molar ratio maintained almost unchanged, as shown in Figure 4.14. It can be inferred that at a higher input voltage, more energetic electrons substantially promote plasma-chemical dehydrogenation reactions and coupling reactions of active species for being converted into H_2, C_2H_2, and C_2H_4. Nevertheless, with increasing input voltage, the C_4H_{10} selectivity remained unchanged, suggesting that the coupling reaction of active species to produce C_4H_{10} was independent of input voltage. Moreover, the CO selectivity initially increased with increasing input voltage from 13.5 to 15 kV and then slightly declined, whereas the H_2/CO molar ratio showed the opposite trend. As mentioned above, the higher the input voltage, the higher the electron density, leading to not only more CO_2 dissociation reactions (Equations 4.1-4.3) but also more CO dissociation reaction (Equation 4.3). Therefore, with further increasing input voltage from 15 to 16.8 kV, the CO selectivity tended to slightly decrease.

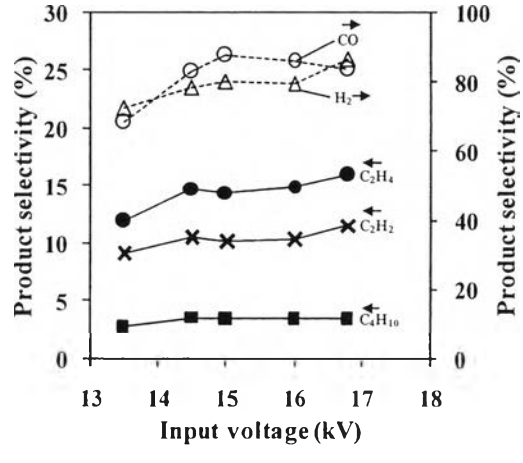

Figure 4.13 Effect of input voltage on product selectivities for the combined steam reforming and partial oxidation of natural gas (3 stages of plasma reactors; steam content, 10 mol%; HCs/O_2 feed molar ratio of 2/1; total feed flow rate, 100 cm^3/min; input frequency, 300 Hz; and electrode gap distance, 6 mm).

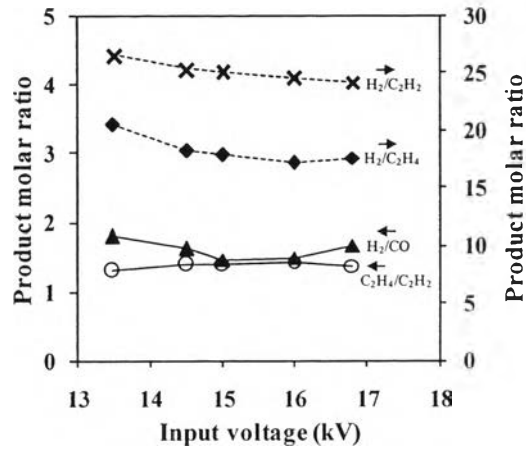

Figure 4.14 Effect of input voltage on product molar ratios for the combined steam reforming and partial oxidation of natural gas (3 stages of plasma reactors; steam content, 10 mol%; HCs/O_2 feed molar ratio of 2/1; total feed flow rate, 100 cm^3/min; input frequency, 300 Hz; and electrode gap distance, 6 mm).

4.3.3 Effect on Power Consumptions and Coke Formation

The effect of input voltage on the power consumptions and coke formation is illustrated in Figure 4.15. The results reveal that with increasing input voltage form 13.5 to 15 kV, the power consumptions both per reactant molecule converted and per H_2 molecule produced decreased drastically. The results can be described by the sharp increases in both CO_2 conversion and H_2 yield. The same explanation can be used to explain the slight changes in both power consumptions per reactant molecule converted and per H_2 molecule produced from input voltage of 15 to 16.8 kV. The increasing tendency in coke formation with increasing input voltage suggests that the CO dissociation reaction favorably occurred at a high input voltage. From the results, the input voltage of 15 kV with the lowest power consumptions was considered to be an optimum value for the combined plasma steam reforming and partial oxidation of CO_2-containing natural gas in a multistage gliding arc system in this present work.

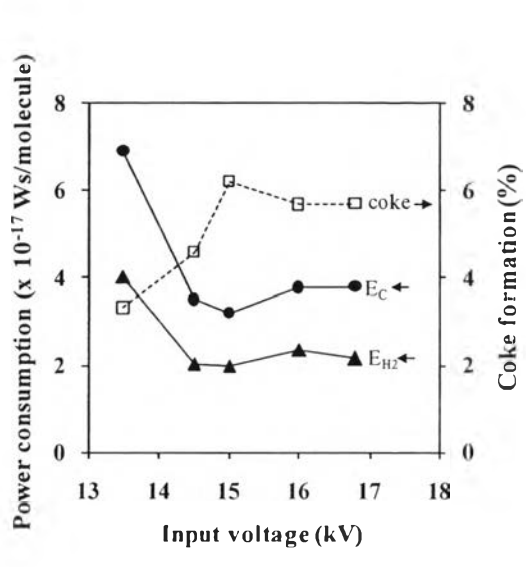

Figure 4.15 Effect of input voltage on power consumptions and coke formation for the combined steam reforming and partial oxidation of natural gas (3 stages of plasma reactors; steam content, 10 mol%; HCs/O_2 feed molar ratio of 2/1; total feed flow rate, 100 cm^3/min; input frequency, 300 Hz; and electrode gap distance, 6 mm).